# New fused bis-thienobenzothienothiophene copolymers and their use in organic solar cells and transistors.

Laure Biniek[1,3*], Bob C. Schroeder[1], Jenny E. Donaghey[1], Nir Yaacobi-Gross[2], Raja Shahid Ashraf[1], Ying W. Soon[1], Christian B. Nielsen[1], James R. Durrant[1], Thomas D. Anthopoulos[2], and Iain McCulloch[1]

[1]*Department of Chemistry and Centre for Plastic Electronics, Imperial College London, London SW7 2AZ, UK*

[2]*Department of Physics and Centre for Plastic Electronics, Imperial College London, London SW7 2AZ, United Kingdom*

[3]*Institut Charles Sadron, CNRS-Université de Strasbourg, 23 rue du Loess, 67034 Strasbourg, France*

## ABSTRACT

A new tetradodecyl-substituted DTBTBT donor unit is synthesised by a specific bis-annulation by Suzuki–Miyaura coupling and successfully incorporate into light absorbing electron donor copolymers for OPV and hole and electron transport OFET polymer devices. All copolymers (DTBTBT-co- Benzothiadiazole (Bz), DTBTBT-co-Thiophene (T) and DTBTBT-co-thienothiophene (TT)) show fully coplanar backbone and strong intermolecular interactions. The DTBTBT-Bz copolymer led to a deep HOMO level (-5.2 eV) and thus a large $V_{oc}$ value of 0.92 V with $PC_{71}BM$ as electron acceptor and a PCE of 3.7 % with a $J_{sc}$ of 6.78 mA/cm$^2$ could be obtained. A hole mobility of 0.1 cm$^2$/Vs has been observed for the highly coplanar and more crystalline DTBTBT-T copolymer.

## INTRODUCTION

Molecular engineering of organic semiconductors has played an essential role in the improvement of organic electronic devices performances. In particular, the design and development of a large range of different conjugated polymers, focused on improving the optical absorption, planarizing the aromatic backbone and therefore adjusting the molecular orbital energy levels, has lead to an improved understanding of the structure-properties relationships.[1-5] Most of the highest performing polymers show short pi-stacking distances between polymer backbones with wave functions often widely delocalized over the polymer conjugated aromatic system.[6] These properties, leading to high charge carrier mobilities, have often been obtained with ring fusion of heteroarenes.[7-10]

Herein we have designed and synthesised an extended and soluble tetradodecylthieno[3',2':6,7][1]benzothieno[3,2-*b*]thieno[3,2-*g*][1]benzothiophene core unit (DTBTBT, Scheme 1) which was incorporated into light absorbing electron donor copolymers for OPV and hole and electron transport OFET polymer devices. The two outer thiophene rings whose acidic 2-positions are easy to functionalize, facilitate the incorporation of the heteroarene unit into polymers via various cross-coupling schemes. Additionally, these thiophene rings offer low steric distortion to the backbone planarity, i.e. a small dihedral angle, when they are coupled into a polymer chain, which should be advantageous for close packing in the solid state and provide the basis for interesting electronic properties.[5] The proposed synthesis pathway allows the introduction of four lateral alkyl side chains onto the ladder-type monomer, which promotes good solubility and processability. The alkyl chains are attached to the aromatic ring system via a $sp^2$-hybridized carbon, thus project coplanar to the polymer backbone, in contrast to the case of $sp^3$-hybridized carbons for which the alkyl chains protrude out of the plane of the polymer backbone[11] which should be advantageous for intermolecular interactions.

The new electron-rich monomer was copolymerized with three different co-monomers, the electron-deficient 2,1,3-benzothiadiazole (Bz) and two electron-rich units, thiophene (T) and thieno[3,2-*b*]thiophene (TT) respectively. The choice of electron-deficient and -rich co-monomers allows us to evaluate the potential of the new DTBTBT unit in both organic photovoltaic and transistor devices.

In the following, the synthesis, optical, electrochemical and morphological properties are presented and the performance of organic solar cells and organic transistors devices are discussed.

## EXPERIMENTAL SECTION

**Materials.** All chemicals were purchased from commercial suppliers unless otherwise specified. The synthesis of the 2,2'-(13Z)-hexacos-13-ene-13,14-diylbis(4,4,5,5-tetramethyl-1,3,2-dioxaborolane) (**2**) and 2,8-dibromo-4,5,10,11-tetradodecylanthra[1,2-*b*:5,6-*b'*]bisthiophene (**6**) are described in supporting information.

**4,5,10,11-tetradodecylthieno[3',2':6,7][1]benzothieno[3,2-*b*]thieno[3,2-*g*][1]benzothiophene (3)**. 3,6-dibromo-2,5-bis(3-bromothiophen-2-yl)thieno[3,2-*b*]thiophene **1** (2.0 g, 3.22 mmol), (Z)-1,2-bis(4,4,5,5-tetramethyl-1,3,2-dioxaborolan-2-yl)-1,2-didodecylethene **2** (3.97 g, 6.45 mmol), were dissolved in deoxygenated THF (60 mL). The mixture was then degassed by bubbling nitrogen for 1.5 hours at room temperature before the addition of Pd(dppf)$Cl_2$ (165 mg, 0.22 mmol), (further degassing for 5 min). After degassing for additional 5 minutes, degassed $K_3PO_4$ aq (3M, 10.7 mL) was added. The reaction mixture was refluxed at 80 °C for 2 h and then at 65 °C overnight. The reaction mixture was quenched with water, and extracted with diethyl ether before being washed with water. The

collected organic layer was dried over $MgSO_4$. After removal of the solvent under reduced pressure, the residue was purified by column chromatography on silica gel (hexane) to give a pale yellow solid (762 mg, 21.9 %). $^1$H NMR ($CDCl_3$, 300 MHz, ppm): δ 7.49 (d, J = 5.4 Hz, 2 H), 7.52 (d, J = 5.4 Hz, 2 H) 3.25 (m, 4 H), 3.08 (m, 4 H), 1.73-1.68 (m, 4 H), 1.47-1.29 (m, 4 H), 1.28 (m, 72H), 0.88 (m, 12 H), $^{13}$C NMR (100 MHz, $CDCl_3$): δ 138.05, 133.92, 132.88, 131.98, 131.47, 131.09, 130.55, 124.15, 123.83, 32.09, 31.85, 31.18, 30.58, 30.39, 30.30, 29.87, 29.81, 29.71, 29.54, 22.86, 14.28. MS (MALDI-TOF LD$^+$, $C_{66}H_{104}S_4$): calcd, 1024.7 found, 1025. mp (°C): 113-115.

**2,8-dibromo-4,5,10,11-tetradodecylthieno[3',2':6,7][1]benzothieno[3,2-*b*]thieno[3,2-*g*][1]benzothiophene (4).** 4,5,10,11-tetradodecylthieno[3',2':6,7][1]benzothieno[3,2-*b*]thieno[3,2-*g*][1]benzothiophene **3** (470 mg, 0.46 mmol) was dissolved in $CHCl_3$/Acetic acid (40 mL / 4 mL) under argon in the dark. *N*-bromosuccinimide (173 mg, 0.96 mmol) was added portion wise over 15 minutes. The reaction mixture was stirred overnight at room temperature then quenched with water, extracted with chloroform and washed with water. The collected organic layer was dried over $MgSO_4$. After removal of the solvent under reduced pressure, the residue was recrystallized in a mixture of ethanol and dichloromethane to give a pale yellow solid (530 mg, 97 %). $^1$H NMR ($CDCl_3$, 300 MHz, ppm) δ: 7.43 (s, 2H), 3.15 (m, 4H), 2.96 (m, 4H), 1.68 (m, 8H), 1.51-1.28 (m, 72H), 0.87 (m, 12H). $^{13}$C NMR (100 MHz, $CDCl_3$, ppm) δ: 137.81, 133.01, 132.89, 132.17, 131.65, 131.38, 130.48, 126.58, 113.00, 32.10, 31.78, 31.71, 31.19, 30.51, 30.33, 30.27, 29.88, 29.82, 29.76, 29.68, 29.62, 29.55, 22.86, 14.28. MS (MALDI-TOF LD$^+$, $C_{66}H_{102}Br_2S_4$): calcd, 1182.5 found, 1182.8. mp (°C): 125-128.

**DTBTBT-Bz and DTAT-Bz by Suzuki polymerisation.** A 20 mL microwave vial was charged with monomer **4** or **6** (0.160 g, 1.0 eq), 1.0 eq. of 2,1,3-benzothiadiazole-4,7-

bis(boronic acid pinacol ester) monomer, 2.2 mol% of tris(dibenzylideneacetone)dipalladium(0) and 8.8 mol% of tri(*o*-tolyl) phosphine, a drop of aliquat 336 and toluene (0.03 M). This mixture was degassed with argon for one hour, followed by the addition of degassed $Na_2CO_3$ solution (1.0 M). The resultant mixture was degassed for another 10 minutes then sealed and heated at 120 °C for 48 h. The polymer was precipitated from acidic methanol (HCl + $CH_3OH$), and collected by filtration and washed with methanol. The polymer was further purified by washing via Soxhlet extraction with methanol (24 h), acetone (24 h), hexane (24 h) then dissolved in chloroform. Remaining palladium residues were removed by treating a polymeric chloroform solution with an aqueous sodium diethyldithiocarbamate solution for 2 hours at 50°C under vigorous stirring. Afterwards the organic phase was separated from the aqueous phase and washed several times with water. The polymeric solution was concentrated under reduced pressure and precipitated into cold methanol. The polymer was filtered off and dried under high vacuum for at least 24 hours providing deep blue solids. DTBTBT-Bz (95 mg, 59 %). $M_n$ = 19 kg $mol^{-1}$, $M_w$ = 132 kg $mol^{-1}$. DTAT-Bz. (132 mg, 82 %) $M_n$ = 19 kg $mol^{-1}$, $M_w$ = 46 kg $mol^{-1}$.

**DTBTBT-T and DTBTBT-TT by Stille polymerisation.** An oven dried microwave vial was charged with 2,8-dibromo-4,5,10,11-tetradodecylthieno[3',2':6,7][1]benzothieno[3,2-*b*]thieno[3,2-*g*][1]benzothiophene **4** (90 mg, 0.076 mmol, 1 eq), and 1 eq of 2,5-di(trimethyltin)thiophene (31 mg, 0.076 mmol) or 2,5-di(trimethyltin)thieno(3,2-b)thiophene (35 mg, 0.076 mmol), tris(dibenzylideneacetone)dipalladium(0) (1.53 mg, 1.67 µmol, 2.2 mol %) and tri-*o*-tolylphosphine (2.04 mg, 6.69 µmol, 8.8 mol %). The vial was sealed and dry chlorobenzene (1.1 mL) was added. The reaction mixture was degassed with argon for 30 minutes before being placed in the microwave reactor and subjected to the following heating conditions: 120 °C for 2 minutes, 140 °C for 2 min, 160 °C for 2 min, 180 °C for 40 min. Once the reaction had cooled, the viscous red liquid was precipitated in methanol and filtered

into a Soxhlet thimble. The precipitates were purified by Soxhlet extraction with acetone, hexane and chloroform (24 hours each). The chloroform fraction was stirred with aqueous sodium diethyldithiocarbamate tetrahydrate at 50 °C for one hour, then the organic layer was separated and washed with water. The chloroform fraction was further purified by preparative scale size exclusion chromatography to remove the low molecular weight fractions. The recovered polymer solution was concentrated under reduced pressure and precipitated into methanol. After filtration the polymer was isolated as a dark red solid (42 mg, 49 %). DBTBT-T. (42 mg, 49 %) Mn = 29 kg $mol^{-1}$, Mw = 77 kg $mol^{-1}$. DBTBT-TT. (33 mg, 37 %) Mn = 9.5 kg mol, Mw = 17 kg $mol^{-1}$.

**Characterizations.** $^{1}H$ NMR and $^{13}C$ NMR spectra were recorded on a Bruker 400 spectrometer in $CDCl_3$ solution at 298 K unless, polymers $^{1}H$ NMR were recorded on a Bruker DRX400. Number-average ($M_n$) and weight-average ($M_w$) molecular weights were determined with an Agilent Technologies 1200 series GPC in chlorobenzene at 80 °C, using two PL mixed B columns in series, and calibrated against narrow polydispersity polystyrene standards. The polymers were additionally purified on a Shimadzu preparative scale size exclusion chromatography system using chlorobenzene as eluent and an Agilent PLgel 10μm MIXED-D column at 80°C. Mass spectra were recorded by the Imperial College London Department of Chemistry Mass Spectrometry Service on a Micromass Platform II or AutoSpec-Q spectrometer. UV-Vis absorption spectra were recorded on a UV-1601 Shimadzu UV-Vis spectrometer. Photo Electron Spectroscopy in Air (PESA) measurements were recorded with a Riken Keiki AC-2 PESA spectrometer with a power setting of 5 nW and a power number of 0.5. X-ray diffraction patterns of thin films deposited on the Si/SiO2 substrate were obtained with a PANALYTICAL X'PERT-PRO MRD diffractometer equipped with a nickel-filtered Cu $K\alpha_1$ beam and a X' CELERATOR detector, using a current of 40 mA and an accelerating voltage of 40 kV. DSC experiments were carried out

with a TA Instruments DSC Q20 and TGA plots were obtained with a Perkin Elmer Pyris 1 TGA. The morphology of polymer: $PC_{70}BM$ blend was observed by TEM. The blend films on ITO/PEDOT:PPS substrate were floated on a 10wt% aq HF solution and recovered on TEM copper grids. TEM was performed in bright field and diffraction mode using a Philips CM12 microscope equipped with a MVII CCD camera (Soft Imaging System; CDD= charge-coupled device).

**Fabrication and characterization of solar cells.** All organic photovoltaic devices have a conventional device architecture, ITO/PEDOT:PSS/Polymer: $PC_{71}BM$/LiF/Al. The precoated ITO glass substrates were cleaned with acetone and isopropyl alcohol under sonification, followed by drying and oxygen plasma treatment. A 30 nm layer of PEDOT:PSS was spin-coated onto the plasma-treated ITO substrate and baked at 150°C for 20 minutes. An 80 nm active layer consisting of blend of polymer and $PC_{71}BM$ dissolved in *o*-dichlorobenzene (ODCB) was spin-coated on the PEDOT:PSS layer and then LiF (2 nm)/Al (120 nm) cathode was finally deposited by thermal evaporation under high vacuum ($10^{-6}$ mbar) through a shadow mask. The pixel size, defined by the spatial overlap of the ITO anode and Li/Al cathode, was 0.045 $cm^2$. The device characteristics were obtained using a Xenon lamp at AM1.5 solar illumination (Oriel Instruments). The photon flux of light incident on the samples was calibrated using a UV-enhanced silicon photodiode. A 590 nm long-pass glass filter was inserted into the beam at illumination wavelengths longer than 620 nm to remove light from second-order diffraction. Photocurrent was measured using a Keithley 2400 source meter; Measurement duration for a given wavelength was sufficient to ensure the current had stabilized (up to around 5 s under low or zero bias light conditions).

**Fabrication and characterization of OFETs.** Top-gate, bottom-contacts (TG-BC) organic field-effect transistors (OFETs) were fabricated onto glass substrate using evaporated bilayer source/drain (S/D) electrodes. These electrodes were made using a 20 nm layer of Al covered

with a sequentially deposited 25 nm thick layer of Au. As deposited electrode structures were then treated with the contact work function modifier monolayer agent pentafluorobenzenethiol (PFBT).[12] The glass/electrodes substrates were then transferred into a nitrogen glove-box in order to complete the remaining device fabrication and electrical characterization stages. Polymer layers were spin-cast from hot (100 °C) ODCB on top of the substrates and annealed at 120 °C for 15 min. The fluoropolymer CYTOP (Ashai Glass) was used as the gate dielectric layer. Device fabrication was completed with the evaporation of the top Al gate electrode by thermal evaporation under high vacuum ($10^{-6}$ mbar).

## RESULTS AND DISCUSSION

### *1. Synthesis of Monomers and Polymers*

Scheme 1 illustrates the synthetic route towards the new DTBTBT unit **3** and the copolymers.

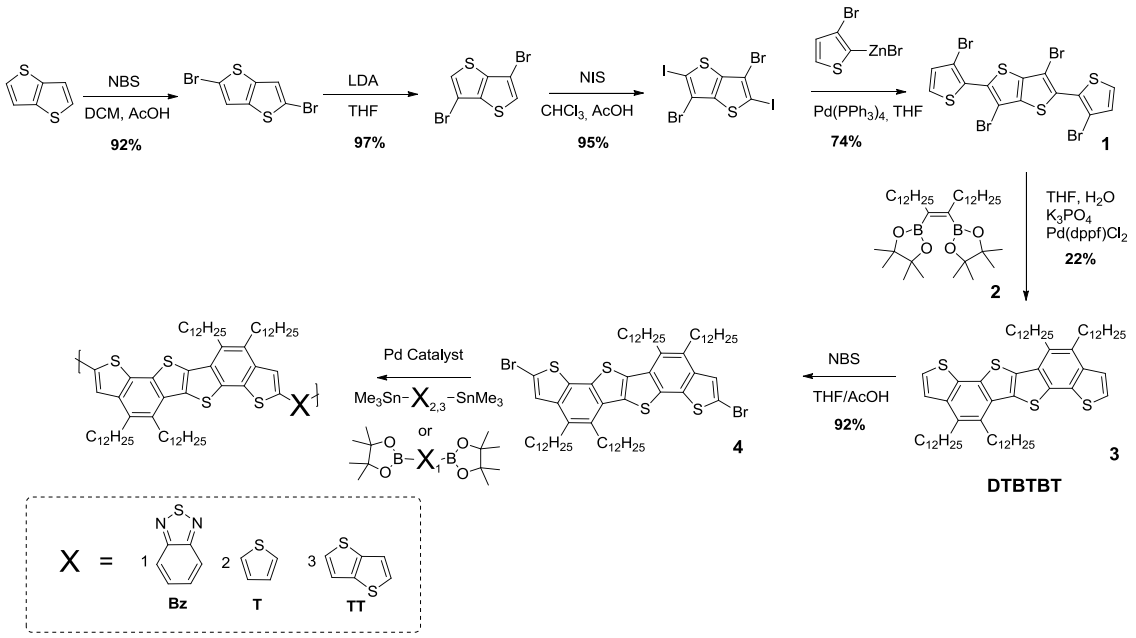


**Scheme 1 : Synthesis pathway towards DTBTBT unit 3 and the three new copolymers.**

In order to get the desired functionalized sp²-carbon bond formation, a specific bis-annulation by Suzuki–Miyaura coupling[13] was used. Indeed, DTBTBT was obtained by a palladium-

catalyzed double cross-coupling reaction of the previously reported tetrabromo-tetraaryl **1**[4] and the vic-diborylated dodecene **2**. This convenient one-pot reaction afforded the new ladder-type monomer **3** in a reasonable yield. The synthesis of the vic-diborylated dodecene **2**, described in the supporting information, could be easily adapted for different kinds of substituents, thus providing a large range of alkylated derivatives.

A subsequent bromination of **3** with *N*-bromosuccinimide provided the final monomer **4** in good yield. Polymer **DTBTBT-Bz** was synthesized via a Suzuki coupling between monomer **4** and 2,1,3-benzothiadiazole-4,7-bis(boronic acid pinacol ester), whereas polymers **DTBTBT-T** and **DTBTBT-TT** were obtained via Stille coupling between monomer **4** and 2,5-bis-(trimethylstannyl)-thiophene or 2,7-bis(trimethylstannyl)-thieno[3,2-*b*]thiophene, respectively.

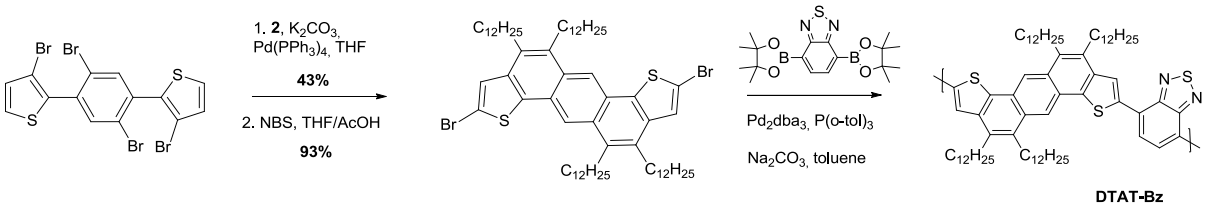


**Scheme 2: Synthesis of the anthradithiophene based polymer DTAT-Bz.**

For comparison, an angular fused anthradithiophene (DTAT) unit was also prepared, which had been independently reported by Wu et al.[14] The desired 4,5,10,11-tetradodecylanthra[1,2-*b*:5,6-*b*']bisthiophene was synthesized in good yield (43 %, Scheme 2) by using tetrakis(triphenylphosphine)palladium as catalyst in combination with potassium carbonate. After bromination of the ring-closed monomer, **DTAT-Bz** polymer was synthesized using the same polymerization condition as **DTBTBT-Bz** to ensure a valid comparison.

All polymers were purified by precipitation from methanol followed by Soxhlet extraction using acetone, hexane and chloroform. The latter fraction was stirred with aqueous sodium

diethyldithiocarbamate to remove residual catalytic impurities. Lower molecular weight fractions of **DTBTBT-T** and **DTBTBT-TT** were removed by recycling gel permeation chromatography (GPC) in chlorobenzene. The number-average molecular weights ($M_n$) of the polymers were evaluated by GPC in chlorobenzene at 80°C to be between 20 to 30 kDa, except for the thieno[3,2-*b*]thiophene derivative (**DTBTBT-TT**) which has a lower $M_n$ of 9 kDa (See Table 1). This lower value might be due to the more planar backbone of the polymer which can easily lead to strong intermolecular interaction and aggregation, thus limiting the polymer solubility and therefore chain growth. All polymers are soluble in hot chlorinated solvent such as chloroform, chlorobenzene (CB) and ortho-dichlorobenzene (ODCB), whereas at room temperature they tend to aggregate and gel in solution.

## Optical Properties and polymer chain conformation

| Polymer | $M_n/M_w$ (kDa) | $\lambda$ max$^{sol}$ (nm)[a] | $\lambda$ max$^{film}$ (nm) | $E_g^{opt}$ (eV)[b] | $E_{HOMO}$ (eV)[c] | $E_{LUMO}$ (eV)[d] | $T_d$ (°C)[e] |
|---|---|---|---|---|---|---|---|
| DTBTBT-Bz | 19/132 | 403/613 | 403/621 | 1.8 | -5.2 | -3.4 | 450 |
| DTBTBT-T | 29/77 | 497 | 496 | 2.2 | -4.9 | -2.7 | 435 |
| DTBTBT-TT | 9/17 | 494 | 494 | 2.2 | -4.9 | -2.7 | 430 |
| DTAT-Bz | 19/46 | 355/582 | 356/634 | 1.8 | -5.3 | -3.5 | 440 |

**Table 1: Properties of the polymers. [a]Values extracted from temperature dependent studies at 85°C. [b]Estimated from the optical absorption edge in thin films. [c]Measured by UV-PESA. [d]Values deducted from $E_{HOMO}$ and optical band gap. [e]Decomposition temperature (5% weight loss) determined by thermal gravimetric analysis under nitrogen.**

The UV-*vis.* absorption spectra of both donor-acceptor alternating copolymers in CB at room temperature and in thin films are shown Figure 1a. The benzothiadiazole based copolymers show two distinct features, a $\pi$–$\pi^*$ transition at higher energy and an internal charge transfer (ICT) transition at lower energy. Interestingly the anthradithiophene **DTAT-Bz** based polymer shows a higher intensity for the $\pi$–$\pi^*$ transition, than for the ICT transition, in contrast to the DTBTBT based polymer. Furthermore, the bandwidth of the transition at lower energy is larger for **DTBTBT-Bz**. This might be explained by a larger overlap of $\pi$ orbitals due to a better packing.[15] In both cases, almost no absorption maximum shift from solution to the solid state is observed, which corroborates the strong aggregation of the polymers in solution. The optical bandgaps extracted from the absorption edges are 1.8 eV for both **DTBTBT-Bz** and **DTAT-Bz**.

The absorption spectra of the electron rich thiophene and thieno[3,2-*b*]thiophene based **DTBTBT-T** and **DTBTBT-TT** polymers are presented in Figure 1b. Their optical properties are similar due to their structural similarity. Again, no shifts of the absorption maxima, around 495 nm, can be observed from solution to thin film corroborating the assumption of strong aggregation of the polymer chains even in dilute solution. However, we note a slight broadening of the absorption towards the lower wavelengths in the case of the TT based polymer probably due to a lower molecular weight. The optical bandgaps extracted from the absorption edges are 2.2 eV for both **DTBTBT-T** and **DTBTBT-TT**.

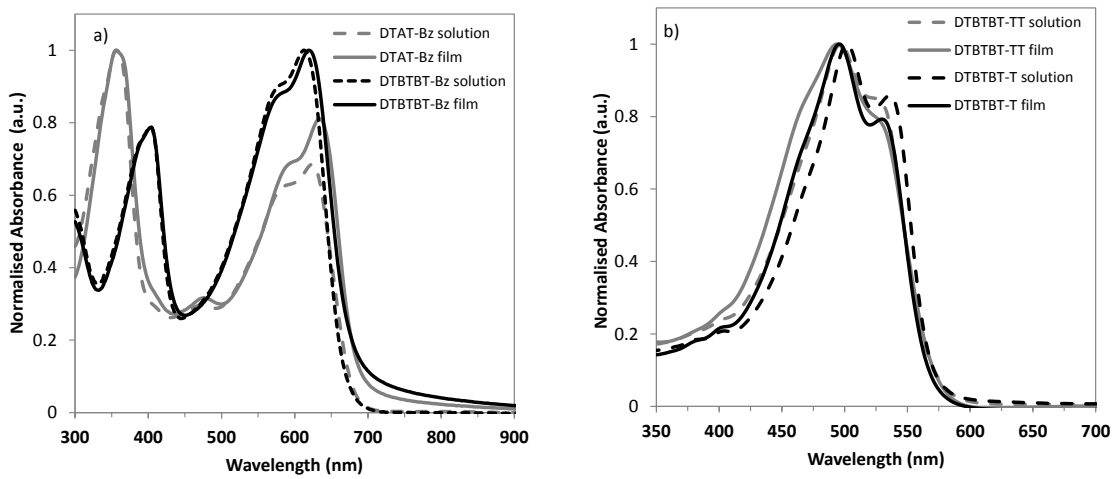


**Figure 1 : Normalised UV-Vis absorption spectra of polymers in CB at 25°C (dashed line) and in thin films (plain line) of a) donor-acceptor alternated copolymers b) thiophene and thienothiophene based polymers.**

The aggregation in solution has been studied by in situ temperature-controlled UV-*vis.* absorption measurements. (Figure I, SI). Upon heating, a change of the absorption spectra is observed most notably for the **DTAT-Bz** polymer with a blue shift of the absorption maximum and a disappearance of the second shoulder at low energy. A clear isosbestic point supports the idea of an aggregate -to -solute conversion upon heating whereas only a slight decrease of the absorption intensity is observed for **DTBTBT-Bz**. It seems more difficult to break up the aggregation in solution for the **DTBTBT-Bz** polymer than for **DTAT-Bz** which confirms a stronger intermolecular interaction of the bis(thienobenzothienothiophene) unit than the anthradithiophene unit.

The minimum energy conformations of the Bz based polymers were calculated via density functional theory (DFT) using the B3LYP/6-31G* model and are represented in Figure 2. Even if both polymers are fully coplanar (torsion angles of 0° and 2° for **DTBTBT-Bz** and **DTAT-Bz**, respectively) we note a less pronounced backbone curvature for **DTBTBT-Bz** polymer compared to the **DTAT-Bz**. This geometrical difference might explain the strongest

tendency of DTBTBT based polymer to aggregate in solution[16] and is also leading to a larger delocalisation of the HOMO energy distribution over the backbone. In this system, the sulphur atoms of the central thienothiophene ring contribute to the highest occupied molecular orbital (HOMO) energy distribution, which should enhance the probability of close orbital interactions between cofacial polymer chains in the solid state, thereby facilitating charge carrier interchain hopping. The anthradithiophene unit presents a slightly disrupted HOMO energy delocalisation probably due to the fact that a fusion of aromatic benzene rings is leading to a decrease of the benzenoid character.[17] Meanwhile the lowest unoccupied molecular orbital (LUMO) energy distribution seems more localised on the benzothiadiazole acceptor unit for **DTBTBT-Bz** than for **DTAT-Bz** supporting the idea of the stronger ICT behaviour observed by UV-Vis spectroscopy.

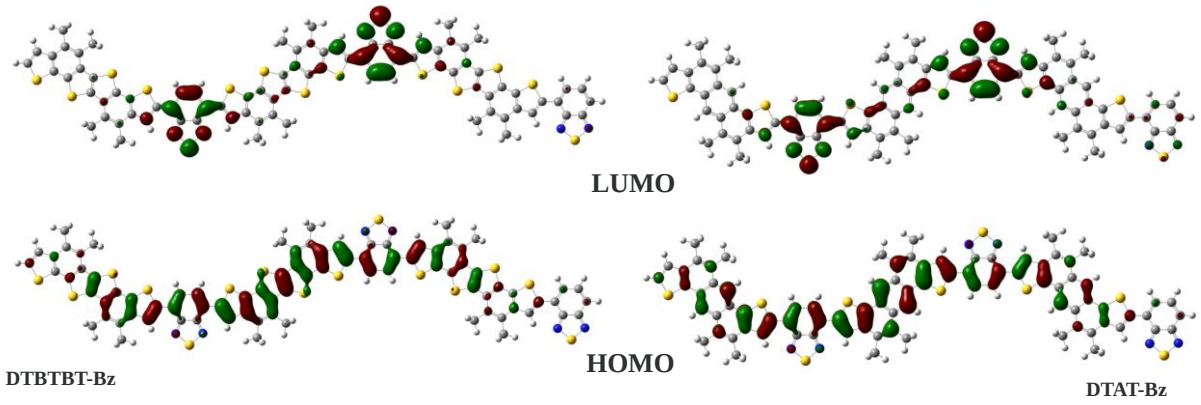


**Figure 2: Minimum energy conformations of trimers of DTBTBT-Bz and DTAT-Bz with their calculated torsion angles. Gaussian optimized at the B3LYP/6-31G* level with visualization of the corresponding HOMO and LUMO energy distributions.**

The copolymerisation of the DTBTBT unit with thiophene (T) or thienothiophene (TT) lead to slightly different polymer backbone conformations as shown in Figure 3. While the TT based trimer is almost fully co-planar, the **DTBTBT-T** shows a slight backbone curvature. However in both cases the very small torsion angles highlight the coplanarity of these new

ladder type polymers. The calculated HOMOs and LUMOs (Figure II, SI), are delocalized over the entire conjugated backbone for both systems. The HOMOs are predominantly aromatic in nature, whereas the LUMOs for both polymers are mainly of a quinoidal character. The good wave-function delocalization and the coplanarity should facilitate both intra- and intermolecular charge transport.

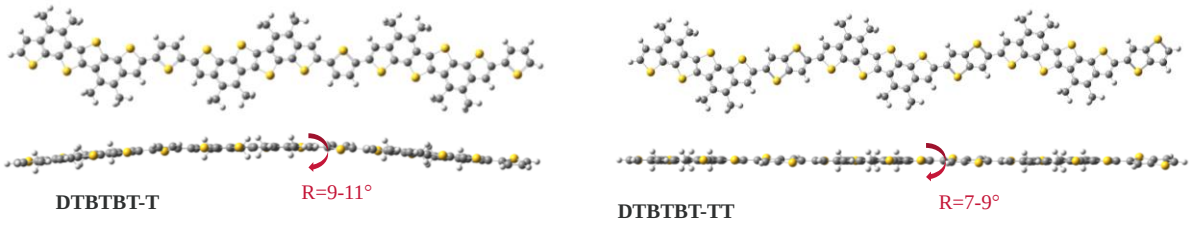


**Figure 3 : Minimum energy conformations of trimers of DTBTBT-T and DTBTBT-TT with their calculated torsion angles.**

## Polymer Energy Levels

The HOMO energy levels of the polymers were measured by photoelectron spectroscopy in air (UV-PESA; see Table 1) and values of -5.2 and -5.3 eV were found for **DTBTBT-Bz** and **DTAT-Bz**, respectively. The slightly higher value for the DTBTBT based polymer might be due to the more electron rich thienothiophene inner ring. The LUMO energy levels were subsequently estimated from the optical band gaps and the HOMO levels; values of -3.4 eV for **DTBTBT-Bz** and -3.5 eV for **DTAT-Bz** were obtained. In the case of the **DTBTBT-T** and **DTBTBT-TT** polymers, higher HOMO and LUMO levels at -4.9 eV and -2.7 eV respectively have been measured. These values are in good agreement with the calculated ones, -4.8 eV for the HOMO levels and -2.6 eV for the LUMO levels of both polymers. We stress that the observed tendencies for aggregation imply that the thin-film morphology of these materials can vary greatly with processing conditions (choice of casting technique,

solvent, temperature, and concentration). Since the morphology can affect both UV-PESA and UV-vis measurements, the values obtained for the frontier-orbital energy levels must be regarded as estimated values.

**Thermal Properties**

All polymers show good thermal stability with decomposition temperatures above 400 °C. No phase transitions were observed by DSC in the temperature range between 60 and 295 °C at a heating rate of 20 °C/min for all polymers. However X-ray diffraction measurements revealed out of plane reflections attributed to lamellar type crystallinity for all films drop-casted on silicon substrates as illustrated in Figure 4. The lamellar and the π–π stacking distances, summarised in Table 2, are slightly shorter in the case of bis(thienobenzothienothiophene) than for the anthradithiophene based polymer supporting the idea that the DTBTBT unit is favouring stronger intermolecular interaction than the DTAT moiety.

A higher degree of crystallinity and a shorter π–π stacking distance (3.6 Å) can be observed for the thiophene and thienothiophene based polymers, as compared to the Bz copolymers, probably due to a better organization of the polymer chains due to their smallest backbone curvature, which should be beneficial for the charge transport properties. An increase in crystallinity upon annealing can be observed in **DTBTBT-T** and **DTBTBT-TT**.

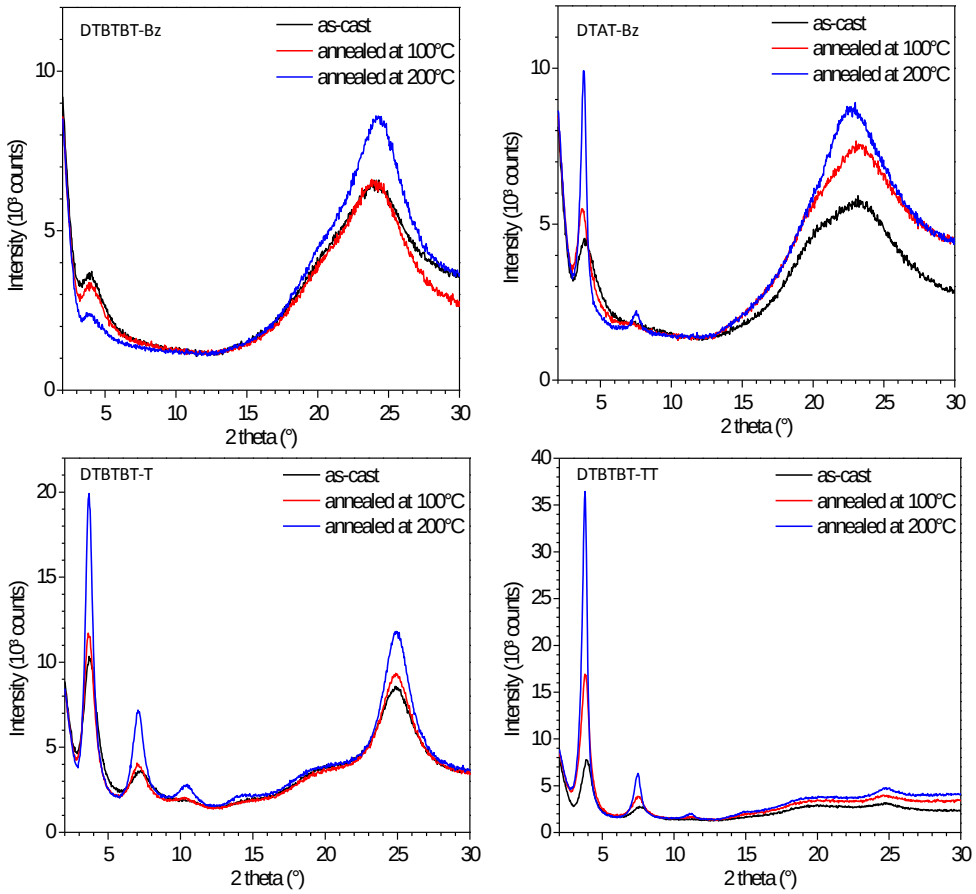


**Figure 4: X-Ray Diffraction (XRD) patterns of drop-casted films of polymers on Si/$SiO_2$ substrates as-cast, annealed at 100°C and 200°C.**

| Polymers | As cast | | 100°C | | 200°C | |
|---|---|---|---|---|---|---|
| | $d_L$ (Å) | $d_\pi$ (Å) | $d_L$ (Å) | $d_\pi$ (Å) | $d_L$ (Å) | $d_\pi$ (Å) |
| DTBTBT-Bz | 22.1 | 3.7 | 22.3 | 3.7 | 22.7 | 3.7 |
| DTBTBT-T | 23.5 | 3.6 | 23.9 | 3.6 | 24.2 | 3.6 |
| DTBTBT-TT | 22.7 | 3.6 | 23.1 | 3.6 | 23.3 | 3.6 |
| DTAT-Bz | 22.5 | 3.8 | 23.7 | 3.8 | 23.1 | 3.9 |

**Table 2: Lamellar ($d_L$) and $\pi$-stacking ($d_\pi$) distances determined by XRD.**

## Photovoltaic results

The photovoltaic performances of all polymers were evaluated in bulk hetero-junction solar cells with a conventional device architecture, ITO/PEDOT:PSS/Polymer:$PC_{71}BM$/LiF/Al. and are summarized in Table 3. The highest open circuit voltage ($V_{oc}$) values were obtained with both low-bandgap polymers, **DTAT-Bz** and **DTBTBT-Bz**, which also have the lowest lying HOMO energy levels of all polymers. Despite the high $V_{oc}$ value of 0.94 V, the power conversion efficiency (PCE) of **DTAT-Bz** was limited by the low current (2.7 %). In the case of **DTBTBT-Bz** the current was increased to 6.0 $mA.cm^{-2}$ leading to a higher PCE of 3.2 %. We believe that the better packing and higher absorption range of the DTBTBT unit are responsible for the current increase compared to DTAT. The external quantum efficiency (EQE) spectrum represented in Figure 5 also supports this hypothesis and confirms that more charges are generated in the case of **DTBTBT-Bz**. In order to get an insight into the blend morphology, both polymer:$PC_{71}BM$ blends were investigated by transmission electron microscopy (TEM). Figure IIIa and c (see supporting information) depicts the typical blend morphologies in bright field for **DTBTBT-Bz**:$PC_{71}BM$ (ratio 1:3.5) and **DTAT-Bz**:$PC_{71}BM$

(ratio 1:3.5). For the DTBTBT based system, a clear phase separated morphology is observed with darker features (~150 nm in diameter) ascribed to PCBM domains, which are surrounded by brighter areas attributed to the polymer phase.[18] In contrast, DTAT based blends display a very different morphology without clear phase separation between $PC_{71}BM$ and polymer. Instead, a regular distribution of holes (~100 nm in diameter) is observed; the origin of which is yet not clear. However, this lack of phase separation might be the origin of the lowest devices performances. Regarding electron diffraction, none of the films showed any reflection from the polymers but only Debye-Scherrer ring at 0.46 nm characteristic of PCBM domains.[19] This observation underlines the poor in-plane order of both polymers in these devices. In order to get a more finely intermixed morphology (shown in Figure IIIb, SI), the $PC_{71}BM$ content was reduced and 1% of chloronaphthalene (CN) was added to the active layer blend. The $V_{oc}$ was barely influenced by those modifications; however the short circuit current density (Jsc) and fill factor (FF) were increased, leading to device efficiencies of 3.7 %. In that case, the **DTBTBT-Bz**:$PC_{71}BM$ blend films display more continuous domains, even though the domain sizes are still rather large (~100 nm) which could potentially lead to exciton recombination, thus limiting device performance.

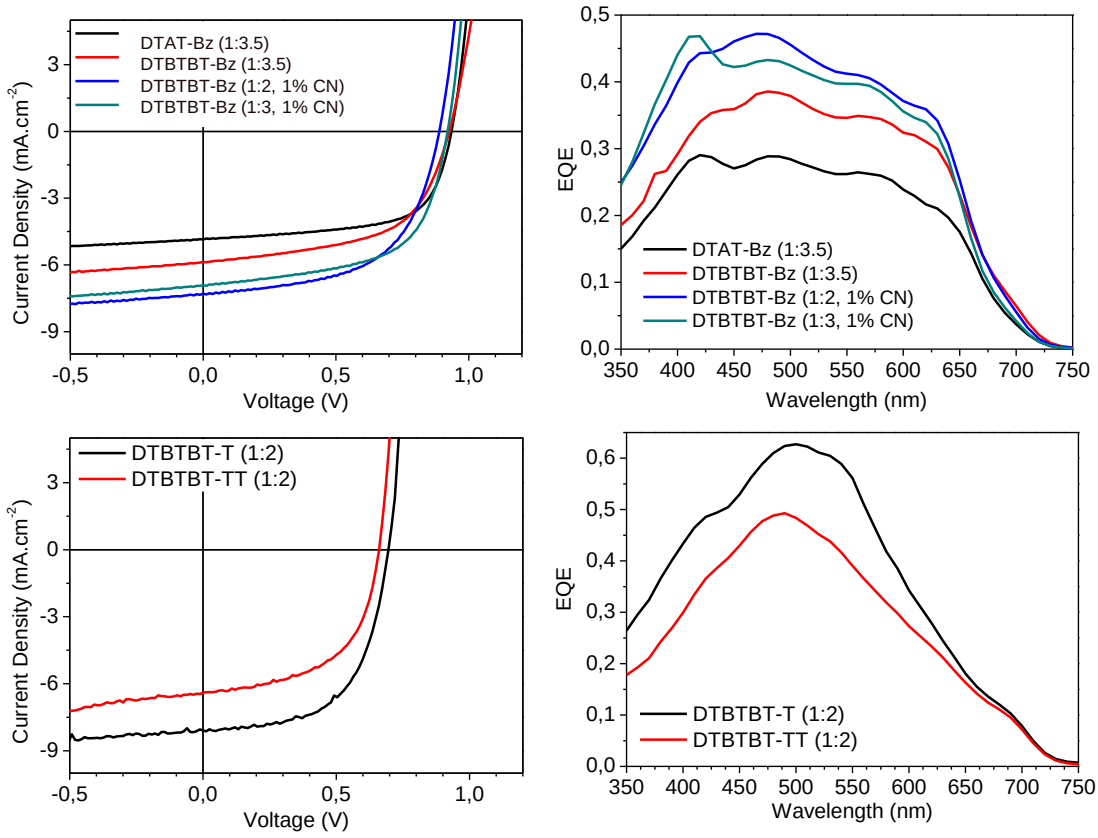


**Figure 5: J-V curves of the solar cells based on polymers/$PC_{71}BM$ under the illumination of AM 1.5, 100 mW/cm$^2$ and the associated EQE.**

Both the thiophene and the thienothiophene copolymers have much higher HOMO energy levels, which is reflected in their lower $V_{oc}$ values. Despite the larger bandgap of these materials and a more limited absorption range, good $J_{sc}$ values and high FFs could be obtained, leading to device efficiencies exceeding 3.3 % for **DTBTBT-T** (Table 3). It is important to note that this value has been obtained without further optimisation of the blend ratio or the active layer morphology. The addition of chloronaphthalene in this case did not improve the performances possibly because of the more crystalline nature of **DTBTBT-T** compared to **DTBTBT-Bz**. The higher backbone coplanarity and higher molecular weight of

the thiophene based polymer might be at the origin of the higher charge generation observed in the EQE and the better charge transport properties leading to better OPV performances.

| P (ratio $PC_{71}BM$) | Jsc ($mA/cm^2$) | Voc (V) | FF | PCE (%) |
|---|---|---|---|---|
| DTAT-Bz (1:3.5) | 4.55 | 0.94 | 0.64 | 2.7 |
| DTBTBT-Bz (1:3.5) | 6.00 | 0.93 | 0.57 | 3.2 |
| DTBTBT-Bz (1:2, 1% CN) | 7.15 | 0.89 | 0.57 | 3.6 |
| DTBTBT-Bz (1:3, 1% CN) | 6.78 | 0.92 | 0.60 | 3.7 |
| DTBTBT-T (1:2) | 8.10 | 0.70 | 0.59 | 3.3 |
| DTBTBT-TT (1:2) | 6.41 | 0.66 | 0.56 | 2.3 |

**Table 3: Photovoltaic properties of DTAT and DTBTBT containing polymers.**

## Field-effect transistor measurements

The charge carrier mobilities were evaluated using top-gate, bottom-contacts (TG-BC) organic field-effect transistors (OFETs) after annealing at 120°C for 15 minutes. Figure 6a and Figure 7a show the transfer characteristics measured for, respectively, **DTBTBT-T** and **DTBTBT-TT** OFET devices. The device based on the thiophene unit exhibit high p-type mobility (~0.1 $cm^2/Vs$). Comparing the thiophene and thienothiophene based polymers reveals a large difference in turn on voltages and while the on/off ratio is comparable (~$10^4$) the hole mobility of the thiophene based polymer is an order of magnitude higher than the thienothiophene one (~0.01 $cm^2/Vs$). The higher hole mobility of **DTBTBT-T** might be explained by its higher molecular weight and slightly lower crystallinity.[20] Close examination

of the output curves (Figure 6b and Figure 7b) at low drain voltages ($V_D$), obtained from the two devices reveals significantly different hole injection characteristics. A significant injection barrier to holes can be seen in **DTBTBT-T** devices. The latter is manifested as a superlinear dependence of drain current ($I_D$) as a function of $V_D$ at low fields. This feature is absent in **DTBTBT-TT** devices, where an Ohmic-like linear dependence of $I_D$ on $V_D$ can be observed. This finding is rather puzzling since photoelectron spectroscopy measurements suggest similar HOMO energy levels for the two polymers (Table 1). Therefore, the apparent injection barrier seen in **DTBTBT-T** devices cannot attributed solely to an energy offset between the electrode work function and the HOMO level, but other factors (e.g. film morphology at the metal and dielectric interfaces) may be responsible.

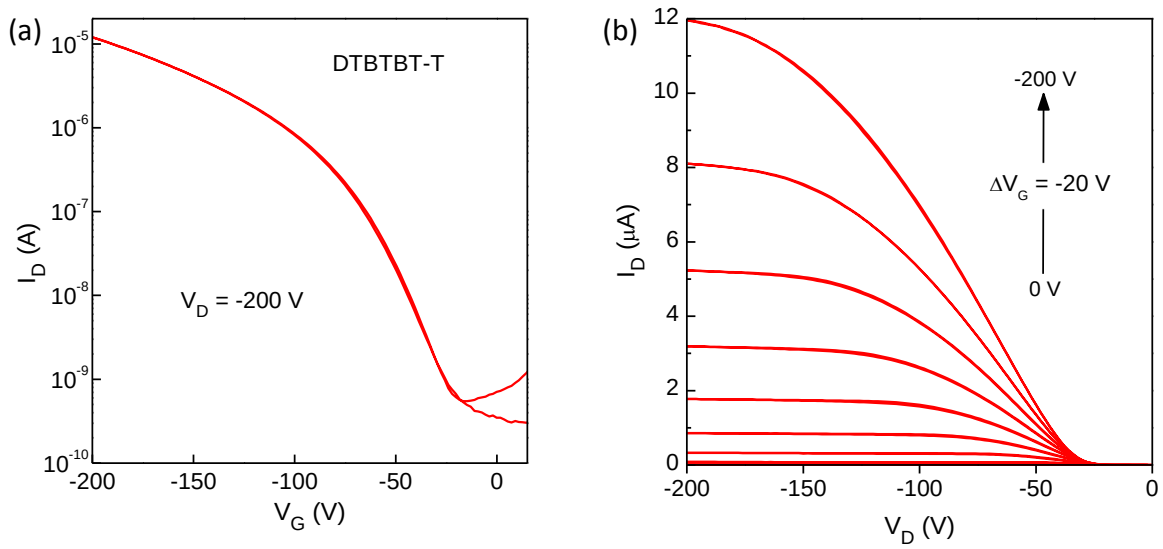


**Figure 6: a) Transfer and b) Output characteristics for the DTBTBT-T OFET. The channel dimensions are length L=20μm and width W=1000 μm.**

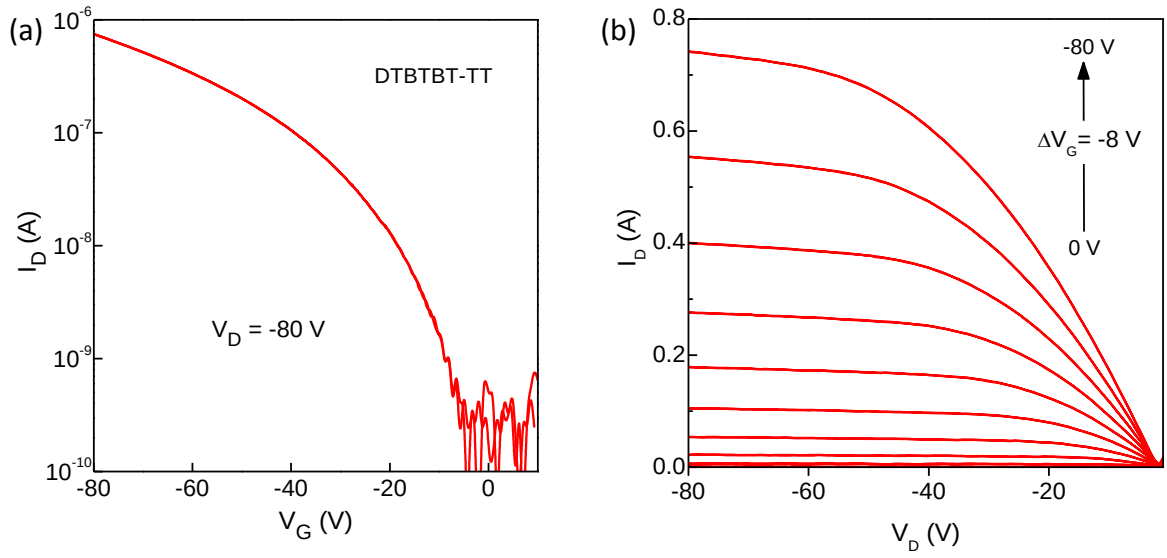


**Figure 7: a) Transfer and b) Output characteristics for the DTBTBT-TT OFET. The channel dimensions are length L=20µm and width W=1000 µm.**

Figure 8a displays a typical set of the transfer characteristics for the **DTBTBT-Bz** transistor. The device exhibits ambipolar characteristic with hole and electron mobilities of ~ 0.01 $cm^2$/Vs and ~0.005 $cm^2$/Vs, respectively. The on/off ratio is relatively low and on the order of $10^3$. The transfer characteristics for the **DTAT-Bz** based transistor are shown in Figure 8b. Again, clear ambipolar charge transport characteristic are observed although the overall performance of the device appears to be lower than the **DTBTBT-Bz** based one probably due to the more pronounced backbone curvature of the DTAT based material. A maximum hole and electron mobilities around ~0.005 $cm^2$/Vs and ~0.001 $cm^2$/Vs, respectively and a channel current on/off ratio in the order of $10^2$ is obtained for **DTAT-Bz**. The low hole mobility might also be at the origin of the low short circuit current observed in DTAT-Bz:$PC_{71}BM$ solar cells. The ability to inject and accumulate both type of carriers (i.e. holes and electrons) within the transistor channel is attributed to both, the relatively narrow band gap of the polymers as well as to the use of bilayer S/D electrodes that consist of a sequentially deposited low workfunction (Al ~ 4.3 eV) and a high workfunction (Au ~ 5 eV) metals.

These simple but rather versatile bilayer S/D electrodes enable the fabrication of devices with ambipolar injection characteristics. We do note however that further improvement in electron injection and transport would be anticipated through the use of S/D electrodes with even lower work functions (e.g. Ca, Al/LiF). This however is beyond the scope of this work and will be addressed in future investigations.

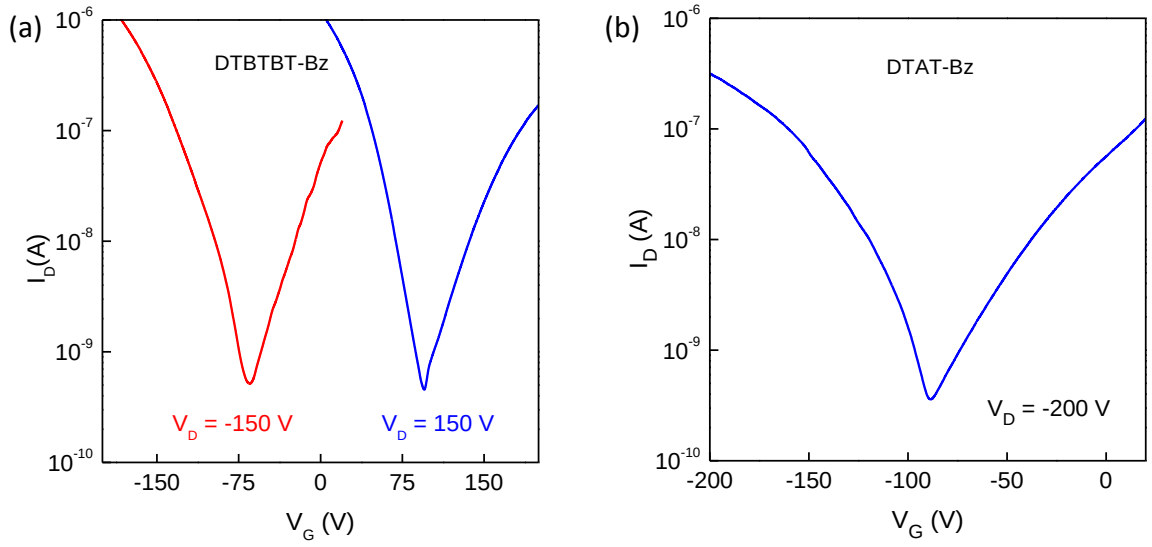


**Figure 8: Transfer characteristics for the DTBTBT-Bz (a) and DTAT-Bz OFETs (b). Both devices have channel dimensions of length L=20µm and width W=1000 µm.**

## CONCLUSIONS

We have successfully synthesized three copolymers of a new tetradodecyl-substituted DTBTBT donor unit and different monomers such as Bz, T and TT by Stille or Suzuki polymerisation. A tetradodecyl-substituted DTAT unit copolymerised with Bz was also synthesized and used as a comparison. The introduction of the alkyl chains in the 2 and 7 positions and the two outer thiophene ring allowed us to incorporate the DTBTBT unit into soluble polymers with good planarity, which were demonstrated to be suitable for both OFET and OPV applications. The **DTBTBT-Bz** copolymer with its electron poor benzothiadiazole

unit led to a deep HOMO level and thus a large $V_{oc}$ value of 0.92 V with $PC_{71}BM$ as electron acceptor and a PCE of 3.7 % with a $J_{sc}$ of 6.78 mA/cm$^2$ could be obtained. A hole mobility of 0.1 cm$^2$/Vs has been observed for the highly coplanar **DTBTBT-T** copolymer. The results indicate that the copolymers based on this new DTBTBT donor unit with optimised alkyl side chains[21] are promising semiconducting polymers for efficient OFET and OPV devices.

## ASSOCIATED CONTENT

*S Supporting Information. Experimental part of intermediates (2), (5) and (6), NMR spectra of monomer 4 and copolymers, Temperature controlled UV-Vis absorption of 4 copolymers in solution, Energy distribution of DTBTBT-T and DTBTBT-TT and Bright field TEM images of typical blends. This information is available free of charge via the Internet at http://pubs.acs.org/.

## AUTHOR INFORMATION

Corresponding Author

*Actual E-mail: laure.biniek@ics-cnrs.unistra.fr

Notes

The authors declare no competing financial interest.

## ACKNOWLEDGMENTS

This work was in part carried out with financial support from Solvay, BASF, SUPERGEN, EC FP7 Project X10D and EC FP7 Project ONE-P, the Centre for Plastic Electronics at Imperial College, Doctoral Training Centre EP/G037515/1, the National Research Fund of Luxembourg and the International Collaborative Research Program of Gyeonggi-do, Korea.

We are grateful to Scott E. Watkins (CSIRO Materials Science and Engineering, Victoria, Australia) for his contribution to the polymer energy levels determination by UV-PESA measurements and to Martin Brinkmann (Institut Charles Sadron, Strasbourg, France) for his great help and constructive discussions on TEM experiments.

## REFERENCES

(1) Chochos, C.L.; Choulis, S.A. *Progress in Polymer Science* **2011**, *36*, 1326-1414.

(2) Son, H.J.; He, F., Carsten, B.; Yu, L. *J. Mater. Chem.* **2011**, *21*, 18934-18945.

(3) Biniek, L; Fall, S.; Chochos, C.L.; Anokhin, D.V.; Ivanov, D.A.; Leclerc, N.; Lévêque, P.; Heiser, T. *Macromolecules* **2010**, *43*, 9779-9786.

(4) Zhou, H.; Yang, L.; You, W. *Macromolecules* **2012**, *45*, 607-632.

(5) Beaujuge, P.M.; Fréchet, J.M.J. *J. Am. Chem. Soc.* **2011**, *133*, 20009-20029.

(6) McCulloch, I.; Asraf, R.A.; Biniek, L.; Bronstein, H.; Comb, C.; Donaghey, J.E.; James, D.I.; Nielsen, C.B.; Schroeder, B.; Zhang, W. *Accounts of Chemical Research* **2012**, *45*, 714-722.

(7) Zhang X.; Johnson, J.P.; Kampf, J.W.; Matzger A.J. *Chem. Mater.* **2006**, *18*, 3470-3476.

(8) Schroeder, B.C.; Ashraf, R.S.; Thomas, S.; White, A.J.P.; Biniek, L.; Nielsen, C.B.; Zhang, W.; Huang, Z.; Shakya Tuladhar, P.; Watkins, S.E.; Anthopoulos, T.D.; Durrant, J.R.; McCulloch, I. *Chem. Commun*. **2012**, *48*, 7699-7701.

(9) Schroeder, B.C.; Nielsen, C.B.; Kim, Y.J.; Smith, J.; Huang, Z.; Durrant, J.; Watkins S.E.; Song, K.; Anthopoulos, T.D.; McCulloch, I. *Chem. Mater*. **2011**, *23*, 4025-4031.

(10) Wang,S.; Kappl, M.; Liebewirth, I.; Müller, M.; Kirchhoff, K.; Pisula, W.; Müllen, K. *Adv. Mater.* **2012**, *24*, 417-420.

(11) Nielsen, C.B.; Turbiez, M.; McCulloch, I. *Adv. Mater.* **2012**, DOI: 10.1002/adma.201201795.

(12) Hamilton, R.; Smith, J.; Ogier, S.; Heeney, M.; Anthony, J.E.; McCulloch, I.; Bradley, D.C.; Veres, J.; Anthopoulos, T.D. *Adv. Mater.* **2009**, *21*, 1166-1171.

(13) Shimizu, M.; Nagao, I.; Tomioka, Y.; Hiyama, T. *Angew. Chem. Int. Ed.* **2008**, *47*, 8096-8099.

(14) Wu, J.-S.; Lin, C.-T.; Wang, C.-L.; Cheng,Y.-J.; Hsu, C.-S. *Chem. Mater*. **2012**, *24*, 2391-2399.

(15) Curtis, M. D.; Cao, J.; Kampf, J.W. *J. Am. Chem. Soc.* **2004**, *126* ,4318-4328.

(16) Rieger, R.; Beckmann, D.; Mavrinskiy, A.; Kastler, M.; Müllen, K. *Chem. Mater.* **2010**, *22*, 5314-5318.

(17) Suresh, C.H.; Gadre, S.R. *J. Org. Chem.* **1999**, *64*, 2505-2512.

(18) Beal, R. M.; Stavrinadis, A.; Warner, J. H.; Smith, J. M.; Assender, H. E.; Watt, A. A. R. *Macromolecules* **2010**, *43*, 2343-2348.

(19) Yang, X.; Van Duren, J.K.J.; Rispens, M.T.; Hummelen, J.C.; Janssen, R.A.J.; Michels, M.A.J.; Loos, J. *Adv.Mater.* **2004**, *16*, 802-806.

(20) Kline, R. J.; McGehee, M. D. *Polym. Rev.* **2006**, *46*, 27-45.

(21) Bronstein, H.; Leem, D.S.; Hamilton, R.; Woebkenberg, P.; King, S.; Zhang, W.; Ashraf, R.S.; Heeney, M.; Anthopoulos, T.D.; de Mello, J.; McCulloch, I. *Macromolecules*, **2011**, *44*, 6649-6652.

**For Table of Contents Use Only**

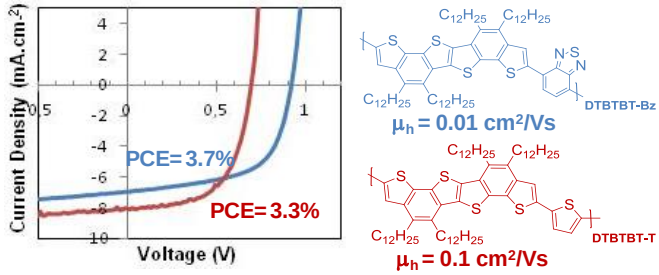


New fused bis-thienobenzothienothiophene copolymers and their use in organic solar cells and transistors.

Laure Biniek, Bob C. Schroeder, Jenny E. Donaghey, Nir Yaacobi-Gross, Raja Shahid Ashraf, Ying W. Soon, Christian B. Nielsen, James R. Durrant, Thomas D. Anthopoulos, and Iain McCulloch.